Research Article

SOHAG JOURNAL OF SCIENCES

https://doi.org/10.21608/sjsci.2024.236449.1123

Comparative Study for the Electrodeposited Cadmium Chalcogenide by Potentiostatic and Potentiodynamic Methods for Electrochemical Reduction of CO_2

Amira Gelany[1,*], Hossnia S. Mohran[1], Mahmoud Elrouby[1,2,*]

[1] *Department of Chemistry, Faculty of Science, Sohag University, Sohag 82524, Egypt.*
[2] *King Salman International University, Faculty of Science, Ras Sudr, 46612, Sinai, Egypt.*
**Email: amira.gelany@science.sohag.edu.eg; dr_mahmoudelrouby@hotmail.com*

Received: 14th September 2023 **Revised:** 10th December 2023 **Accepted:** 1st January 2024
Published online: 30th January 2024

Abstract: Electrochemically synthesized cadmium sulfide (CdS) on cupper-modified substrate from an acidic solution containing Cd^{2+} and $S_2O_3^{2-}$ ions at 20°C has been produced with potentiostatic and potentiodynamic methods utilizing a three-electrode system. The prepared films have been characterized utilizing X-ray diffraction analysis (XRD), scanning electron microscopy (SEM), and energy-dispersive X-ray spectroscopy (EDX). X-ray diffraction analyses demonstrate that, under our optimized conditions, the CdS thin films deposited using both methods exhibit a pure and hexagonal structure. The electrodeposited CdS was found to behave as a p-type semiconductor, which was examined and demonstrated via the Mott-Schottky measurement. Depending upon the obtained data in this work, it was discovered that the electrodeposition techniques affect the morphology of the electrodeposited material (confirmed by SEM), carrier concentrations, thickness δ_{SC} of the space-charge layer, the energy gap (E_g), as well as the sensitivity towards CO_2 electro-reduction.
Keywords: CO_2; Electrochemical deposition; Photo electrochemical; Potentiostatic; Potentiodynamics.

1. Introduction

Cadmium Sulfide (CdS) serves as one of the most significant binary chalcogenides, which is used in different applications such as photosensors, solar cells, gas sensors, semiconductor lasers, electroluminescent photography devices, light-dependent resistances, vacuum ultraviolet (UV) optics, photocatalytic substances, pigment photovoltaic cells, paint industry, piezo transducers, and buffer material for different photovoltaic cells construction [1-5]. This is owing to its advantages: it is a type of semiconductor with an extensive band gap of 2.42 eV at ambient temperature (300°K) [6], possesses hall transportation of the electrons ~104 cm^2 /V s, light transmission <70%, and excellent optical storage capacity [7]. CdS displays a hexagonal or cubic crystal structure with a p-type as well as an n-type depending on the method of preparation or by incorporating some impurities, like (In), (Cl), and (Br). CdS can be produced with different techniques and methods, including pulsed laser beam deposition, sputtering particle beam epitaxy, chemically deposited (CBD), thermally evaporated sol-gel, closer area sublimation, and electrochemical deposition. The highly favored growth method for CdS is the electrodeposition using an aqueous solution due to its accessibility, cheaper growing conditions, flexibility and manufacturability, simplicity of construction, variety of thin films, and production of superior large-area substances in a continuous production method [8-18]. Electrochemical techniques provide a straightforward approach to synthesizing (CdS) under ambient conditions. Common methods include potentiostatic, galvanostatic, and cyclic voltammetry electrochemical deposition on conductive substrates [19]. The morphology can be controlled by tuning factors like solvent, precursors, voltage, temperature, and the use of templates to produce zero-dimensional nanoparticles, one-dimensional nanowires/nanorods, or two-dimensional nanosheets [20]. CdS has been electrodeposited onto various conductive substrates like gold, glassy carbon, fluorine-doped tin oxide (FTO), and titanium dioxide nanotubes, allowing CdS nanostructure integration into photoelectrochemical devices [21]. In this study, the CdS thin films have been generated via electrochemical synthesis from acidic and aqueous solutions using potentiostatic and potentiodynamic methods on a modified substrate with electrodeposited copper. Then, study its electrochemical behavior, photoelectrochemical properties, and electrochemical sensing of CO_2.

2. Experimental

2.1. Chemical and reagents

Cadmium Sulfate ($CdSO_4.8H_2O$), copper (II) sulfate pentahydrate ($CuSO_4.5H_2O$), sodium thiosulphate pentahydrate ($Na_2S_2O_3.5H_2O$), potassium chloride (KCl), tri-sodium citrate, hydrochloric acid (HCl 36%), hydrogen peroxide (H_2O_2 50%), and sulfuric acid (H_2SO_4) were of analytical degree from Sigma, Aldrich, and had been used with no further purification. Each of the solutions was freshly made with double-distilled water at ambient temperature.

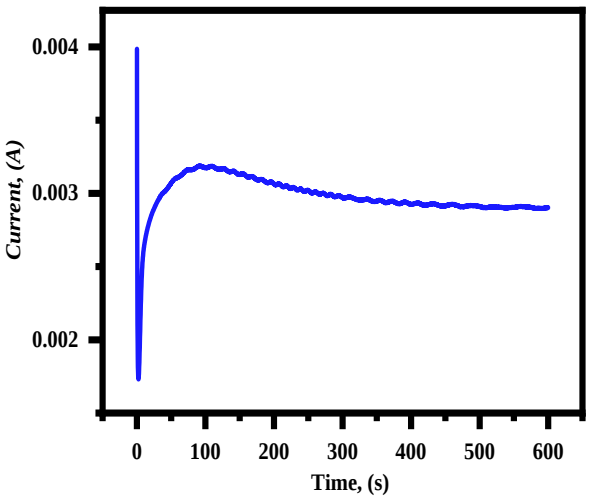

Fig. 1: (Cu) thin film electrodeposition chrono-amperogram on Cu-substrate at ambient temperature (22ºC).

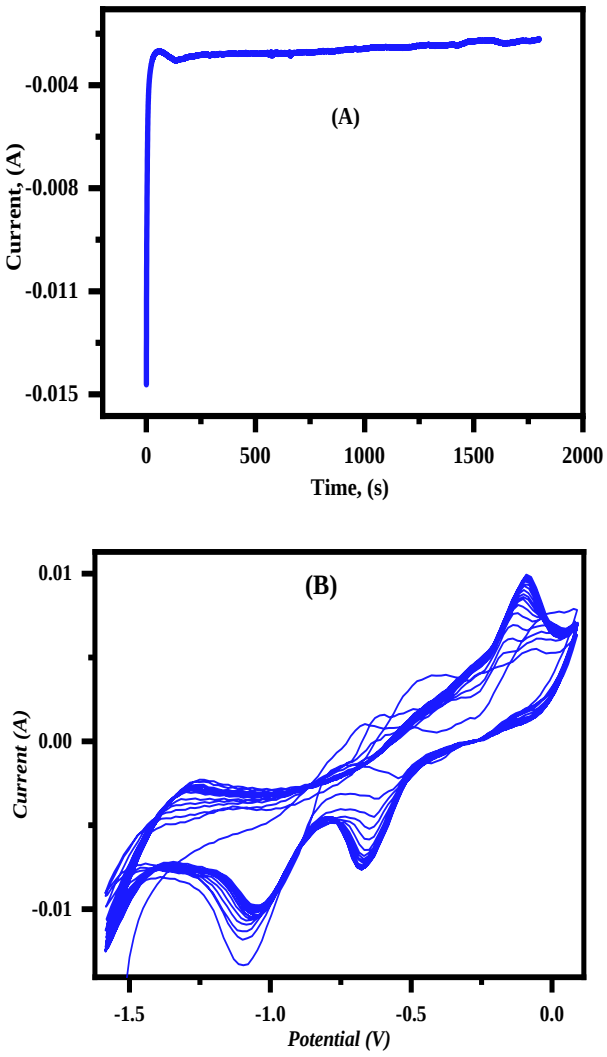

Fig. 2: CdS electrodeposition via (A) chrono-amperogram (potentiostatic mode) at -1.29 V for 30 min and (B) multi-cycle mode at potential range (-1.6 to 0.6) for 30 cycles, at a scan rate of 0.05 Vs^{-1}.

2.2. Instrumentations

Electrochemical investigations were carried out via Versa STAT 4 Potentiostatic/Galvanostatic. A typical three-electrode system was used with an (Ag/AgCl), (Pt), and (Cu) modified sheet (with a surface area of 1 cm^2) used as a reference, counter, and working electrodes, respectively. A digital pH meter has been calibrated by a standard buffer solution. All voltammetric, amperometric, and Mott-Schottky experiments were performed as in the default of the instruments except the potential range and time for each one.

2.3. Preparation of the substrate

1 cm^2 of (Cu) sheet was cleaned via electrochemical polishing solution (H_2SO_4: $3H_2O_2$), respectively. After that, it was washed with double distilled water before experimenting. A copper-thin film was electrodeposited from a solution comprised of 0.01M $CuSO_4.5H_2O$ and 0.1M tri-sodium citrate dissolved in 50 mL of double distilled water using potentiostatic mode at 0.2 V for 600 s vs. (Ag/AgCl) [22]. Then dried at (60ºC) for 20 min.

2.4. Preparation of CdS

The CdS thin films were deposited on thoroughly cleaned Cu-modified substrates using the potentiostatic method at -1.29 V for 30 min. Then, it is followed by potentiodynamic mode at a potential range of (0.1 to -1.6) V for 30 cycles vs. (Ag/AgCl), at (pH = 2.5). The chemical bath involves 0.01M $CdSO_4.8H_2O$, 0.01M $Na_2S_2O_3.5H_2O$, and 0.1M KCl. The nitrogen gas is purged to remove the dissolved oxygen gas from the solution.

3. Results and Discussion

3.1. Cu-substrates preparation

The (Cu) thin film was electrodeposited on a (Cu) sheet from a chemical bath containing 0.01 M Copper (II) Sulfate pentahydrate and 0.1 tri-sodium citrate at a constant potential of 0.2 V for 10 min at ambient temperature (22ºC). Then, it was dried at (60ºC) for 20 min to increase (Cu) thin film stability on the substrate. The (Cu) thin film was electrodeposited to increase the surface activity for CdS electrodeposition. Fig. 1 shows a chrono-amperogram for the potentiostatic deposition of (Cu). As noted in Fig. 1, the current at the beginning decreases rapidly due to the difference between the equilibrium potential of the cell and the applied potential, then increases with time to a limited value, indicating (Cu) well deposition [2, 23].

3.2. Electrodeposition of CdS

Fig. 2 (A) and (B) show the chrono-amperogram and multi-cycle graph, respectively, of CdS deposited on Cu-modified substrate at (pH = 2.5) from a chemical bath containing 0.01 M Cd^{2+}, 0.01M $S_2O_3^{2-}$ and 0.1M KCl at (22ºC) at -1.29 V for the potentiostatic method and a potential range of (-1.6 to 0.6) V for the potentiodynamic method. The figure shows that during the chrono-amperometric deposition and bypassing the time, the current sharply increases to its maximum in the positive direction. Then, as time eclipsed, the current became constant. The sharp increase can be interpreted as a faster or easier

deposition of CdS on copper. This can be caused by a larger concentration of Cd^{2+} and $S_2O_3^{2-}$ or a stronger affinity of the CdS for the new copper surface.

From Fig. 2 (B), two peaks could be observed, one at -0.67, corresponding to thiosulfate reduction, and the other one at -1.09V, corresponding to cadmium sulfide deposition [2, 23].

The mechanism of the electrodeposition in the presence of acidic media is as follows:

$S_2O_3^{2-} + 6H^+ + 8e^- \rightarrow 2S^{2-} + 3H_2O$ (electrochemical reaction) - reversible peak

Sulfide ions near the polarized electrode (negatively) attached with positive ions of Cd^{2+} the reaction takes place easily on the electrode surface, as follows;

$Cd^{2+} + S^{2-} \rightarrow CdS$ (chemical reaction) - irreversible peak

3.2.1. XRD analysis for characterization of the electrodeposited CdS

Fig. 3 illustrates the XRD structures obtained from the electrodeposited cadmium sulfide film by chrono-amperometric and multi-cyclic techniques, as described above, as well as the XRD patterns of the Cu-substrate mentioned in Fig. 3 (a). A comparison between the two preparation methods using the XRD for the deposited cadmium sulfide electrodes generated by the chrono-amperometric and multi-cycle methods is depicted in Fig. 3 (b) and (c), respectively. The patterns are compared to the typical JCPDS no 00-044-0706, 00-004-0836, 01-078-0653, and 01-075-0581, for (CuO), (Cu), (CdO), and (CdS) data sheets, respectively. It was found that the CdS thin film generated by the potentiostatic method is pure CdS but the CdS obtained by multi cyclic method has traces of CdO. Additionally, the X-ray diffraction data revealed that CdS obtained through both methods possesses a hexagonal crystal structure. The figure displays that the substrate intensity peak in the multi-cycle method is lower than that in the potentiostatic method, which can be interrupted by the CdS thin film thinks.

3.2.2. Morphology of the electrochemically synthesized CdS

The morphological characteristics of the CdS thin films electrodeposited on Cu-modified substrate by potentiostatic and potentiodynamic methods are shown in Fig. 4 (a) and (b) were studied using Scanning electron microscopy (SEM). According to Fig. 4 (a), the CdS deposited with the potentiostatic method shows a white-colored accumulated spherical definite particle-like structure taken at an operating distance of 11.1 mm as well as a magnification of 5,000 times the actual image size. Whereas Fig. 4 (b) indicates that the CdS deposited with the potentiostatic method grown at previous conditions shows white-colored accumulated destroyed spherical particles recorded at an operating distance of 11.1 mm with a magnification of 5,000 times the actual image size. This difference in morphology confirms that the deposition method affects the active points on the electrode surface and, hence, the electrodeposited particle growth and other physical properties [2, 23].

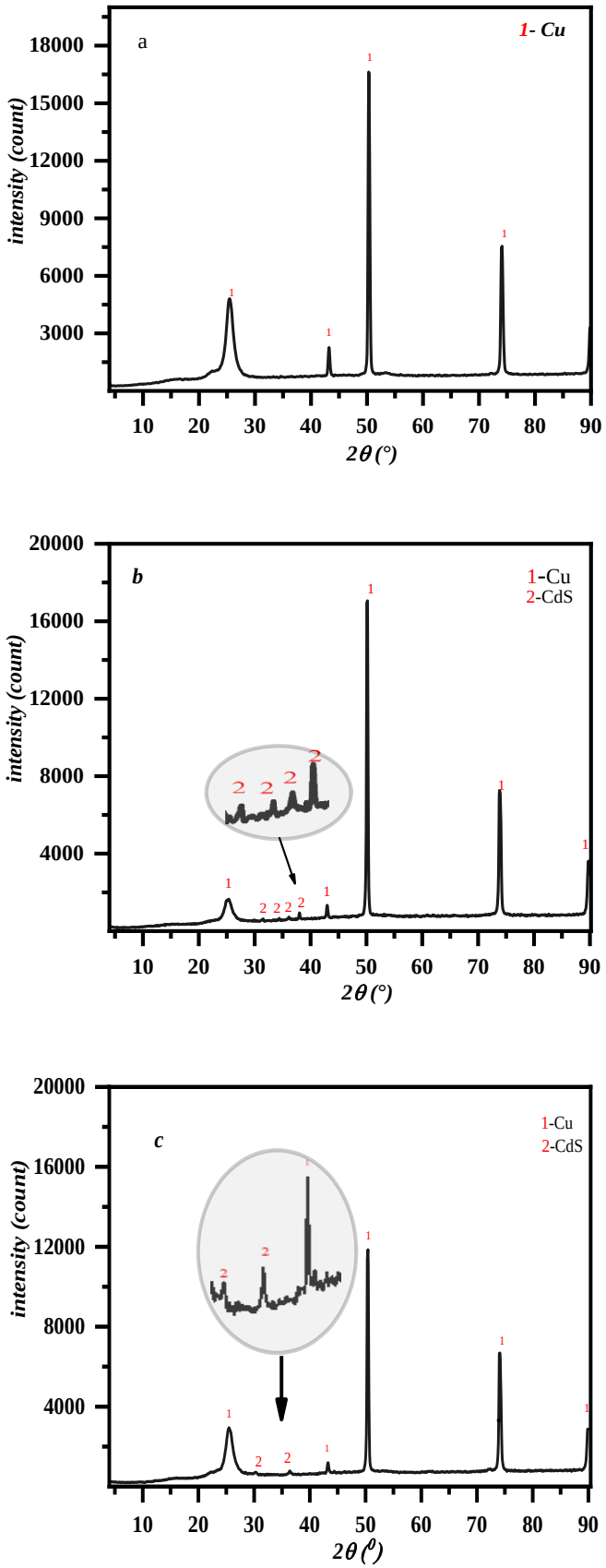

Fig. 3: XRD pattern of (a) Cu-substrate and electrodeposited CdS by (b) potentiostatic mode and (c) multi-cycle mode.

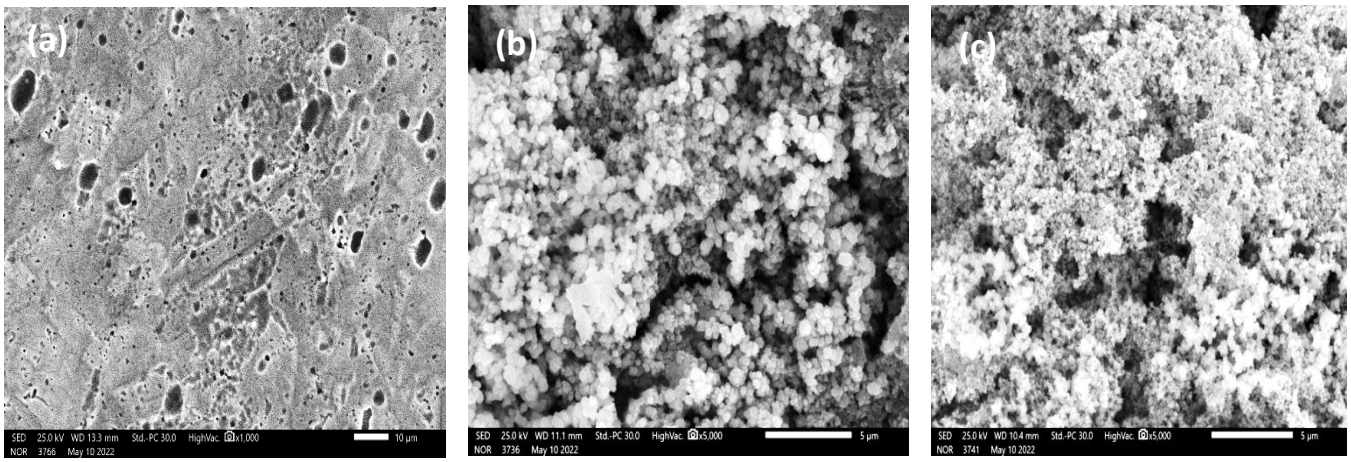

Fig. 4: SEM image (a) Cu-substrate, and CdS thin film deposited by (b) potentiostatic (c) multi-cycle methods.

3.2.3. EDX analysis for identification of the existence of both (Cd) and (S) in the electrodeposited CdS

Fig. 5 shows the typical EDX spectrum of electrodeposited CdS by (a) potentiostatic and (b) multi-cyclic methods, as discussed above. The figure confirms the existence of all (Cd), (S), and so (Cu) with higher (Cd) and (S) content in film deposited with the potentiodynamic technique than that deposited with the potentiostatic technique. The percentage of (Cd) relative to (S) reaches the theoretical value in the potentiostatic method. The atomic percent of (Cd) and (S) in the potentiostatic method were found to be 19.34 and 12.48 respectively. The atomic percent of (Cd) and (S) in the multi-cyclic method were found to be 22.65 and 27.54 respectively.

3.3. Electrochemical measurements

3.3.1. Mott–Schottky spectroscopy

From the Mott-Schottky relationship, more information about the electrodeposits, such as semiconductor type, flat band potential, depletion layer measurement, and number of acceptor carriers. The sample measurement of capacitance performed at 1000 Hz in the potential range from -1 V to 0 V in the cathodic direction is illustrated in Fig. 6 The linear graph of the Mott–Schottky plot in the positive value range of $1/C^2$ reveals the p-type conductive properties of CdS electrode substance.

Extending the plot towards the potential axis provides a measurement of V_{fb} at the point of intercept across the potential axis. Based on the Mott-Schottky relation slope, the concentration of carriers (N_A) in the electrode has been estimated and summarized in Table 1.

$$\frac{1}{C^2} = \frac{2}{\varepsilon\varepsilon_0 e N_D}\left(V - V_{fb} - \frac{kT}{e}\right)$$

where (ε) is the constant of dielectric, (ε_0) is the permittivity in space, (e) is the elementary charge, (ND) is the donor or acceptor quantity, (V) is the voltage applied, (V_{fb}) is the flat band potential, (k) is the Boltzmann constant, and (T) is the temperature in Kelvin. The following equation can be used to determine the thickness (δ_{SC}) of the space-charger layer for p-type semiconductors.

$$\delta_{sc} = \left[\frac{2\varepsilon\varepsilon_0}{eN_D}(V - V_{fb} - \frac{kT}{e})\right]^{\frac{1}{2}}$$

3.3.2. Photoelectrochemical characteristics of the electrodeposited CdS

The photoelectrochemical properties of the p-type electrochemically synthesized cadmium sulfide on Cu-modified substrate by the two methods were investigated in a solution of 0.1 M KCl in a saturated solution of CO_2 at ambient temperature (18°C). Fig. 7 shows the photo-current vs. wavelength relationship for the electrodeposited. cadmium sulfide by (a) potentiostatic and (b) potentiodynamic methods. As appears from Fig. 7 (a), the photocurrent rises along with anodic polarization to its maximum value at 600 nm in the visible light region and then decreases. Whereas in Fig. 7 (b), the maximum value of the photocurrent was in the UV region at 200 nm, then it decreased as wavelength increased

The energy gap (Eg) measurement for the electrode system can be determined by using the value of the maximal photocurrent, which corresponds to λ_{max}. Using the Planck relation, (E = hc/k), the value is found to be 2.07 eV (λ_{max} = 600 nm) and 3.10 eV (λ_{max} = 400) for CdS electrodeposited by potentiostatic and potentiodynamic methods, respectively [2, 23].

Table 1: Capacitance data was recorded for the electrodeposited CdS on modified Cu-substrates.

Electrode	Deposition Method	N_D (cm^3)	V_{fb} (V)	δ_{sc} (cm)
CdS	potentiostatic	5.92×10^{25}	-0.55	5.5×10^{-11}
	Multi-cyclic	8.56×10^{30}	1.13	1.1×10^{-12}

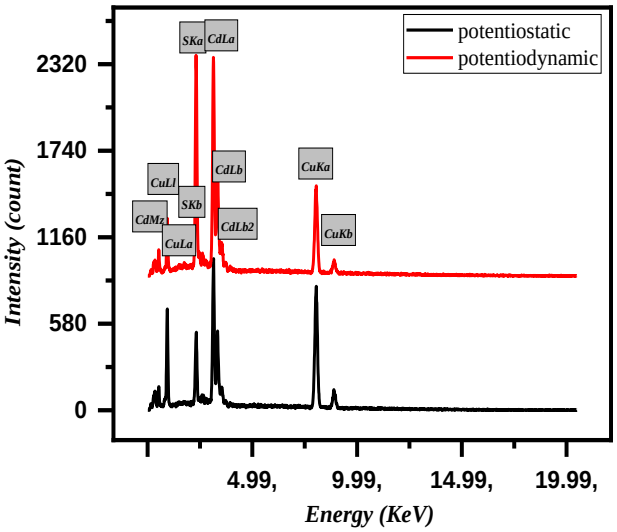

Fig. 5: EDX image of CdS thin film deposited by potentiostatic and multi-cycle method.

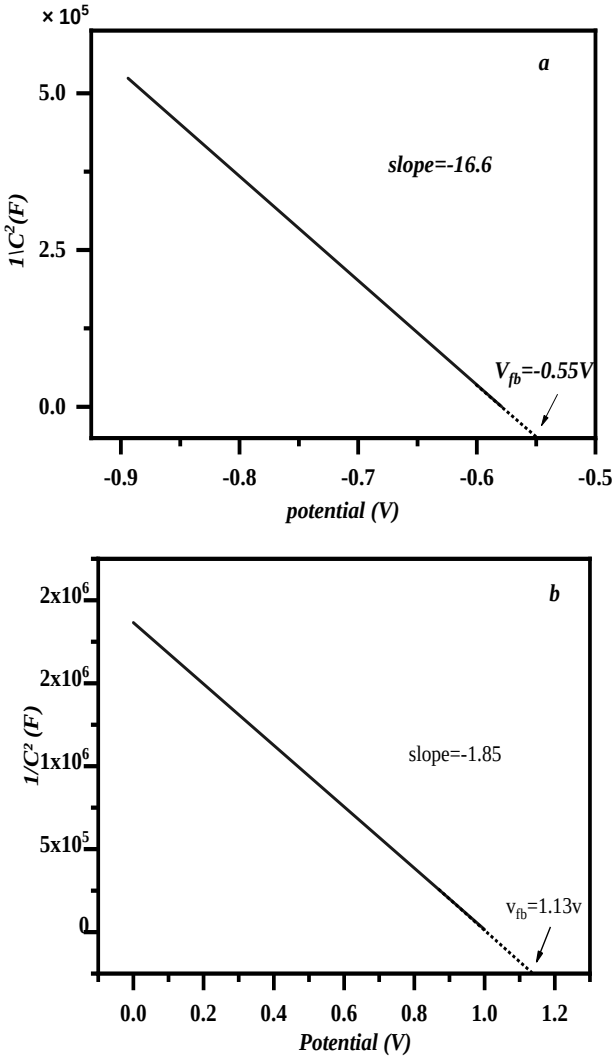

Fig. 6: Mott-Schottky graph of CdS films electrodeposited on Cu from 0.01 M $Na_2S_2O_3$, 0.01 M $CdSO_4.8H_2O$, and 0.1KCl at 1000 Hz, (a) potentiostatic, (b) multi-cyclic method.

3.4. Application

Reduction of CO_2 on the electrochemically deposited CdS

Fig. 8 shows the study of the CO_2 reduction from a solution containing 0.1M KCl in a saturated solution of CO_2 on a CdS electrode prepared by the potentiostatic method at different deposition potentials and the potentiodynamic method prepared at different cycle numbers. Fig. 9 shows the relation between the reduction peak current for CO_2 vs. CdS deposition potential and deposition cyclic number.

From Figs. 8 (a) and 9 (a), it can be noted that the CO_2 reduction peak appeared at -1.16 V at the modified electrode with CdS, which deposited at a deposition potential of -1.1 V, which is the best one of the different deposition potentials. Whereas, in Figs. 8 (c) and 9 (b), the best reduction peak appears at -0.67 V at deposition cycle number 30 cycles, followed by 25 cycles. These results confirm that the CdS deposited by cyclic voltammetry is more catalytic than the other, while the CdS electrodeposited by the potentiostatic method is more sensitive. There is no reduction peak for CO_2 on Cu-substrate as depicted in Fig. 8 (e). The presence of CdS facilitates the electroreduction of CO_2 due to the electron density of S and electron deficiency on C of the CO_2. The electroreduction of carbon dioxide (CO_2) on CdS involves the reduction of CO_2 to form various carbon-containing species, depending on the specific reaction conditions. The overall electrochemical equation for the electroreduction of CO_2 on CdS can be represented as follows:

$$CO_2 + 2H^+ + 2e^- \rightarrow CO + H_2O$$

4. Conclusion

CdS thin films were electrodeposited on a cupper-modified substrate by applying a potentiostatic and potentiodynamic electrodeposition technique at -1.29 V and (0.1 to -1.6) V versus Ag/AgCl/KCl (sat.) for 30 min. and 30 cycles, respectively, in a bath containing 0.1 M KCl, 0.01 M Cd^{2+}, and 0.01 M $S_2O_3^{2-}$ at (pH = 2.5) and (temperature = 20°C). The electrodeposited films produced under the conditions mentioned are pure hexagonal crystals of CdS, as demonstrated by XRD and EDX measurements.

The behavior of the Mott-Schottky plot produced using the two electrodeposition procedures shows that the semiconductor CdS electrodeposited on the Cu-substrate is a p-type semiconductor. The space-charger layer's carrier density (ND), thickness (δ_{SC}), and flat band potential (V_{fb}) were all calculated.

The (Eg) was determined using the i-λ curves and the λ_{max} values and were found to be 2.07 eV (λ_{max} = 600 nm) and 3.10 eV (λ_{max} = 400) for CdS electrodeposited by potentiostatic and potentiodynamic methods, respectively.

CO_2 reduction has been studied using the electrodeposited cadmium sulfide electrodes obtained by the two techniques at different deposition potentials and cycle numbers, and the highest CO_2 reduction efficiency obtained from electrodes deposited at (p = -1.1) and (n = 30) cycles for potentiostatic and potentiodynamic methods.

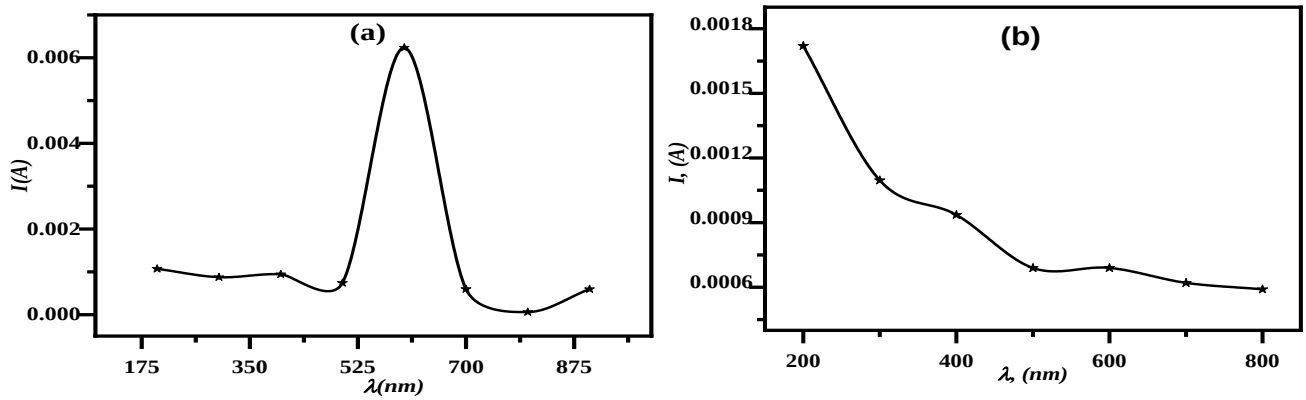

Fig. 7: Plot of photocurrent against λ for CdS under the conditions of contact of light with a spectral composition range of (900 <λ< 200).

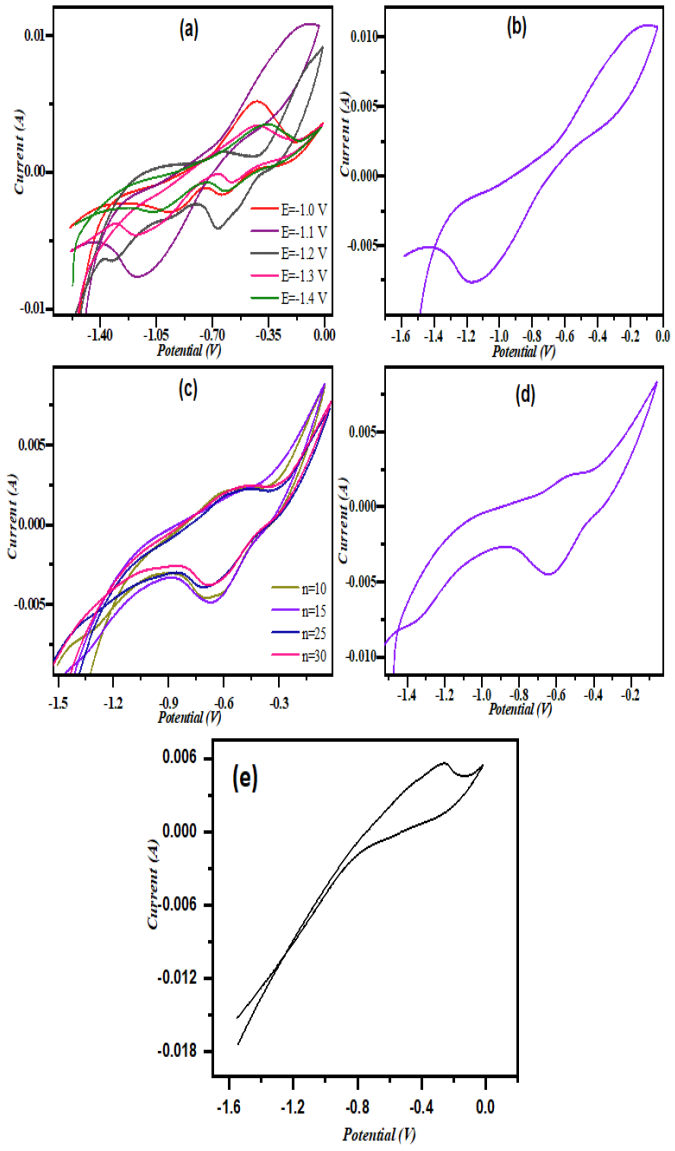

Fig. 8: CV of solution contains 0.1M KCl saturated with CO_2 gas on the electrodeposited CdS by (a, b) potentiostatic (c, d) potentiodynamic method, and (e) the CV of CO_2 in 0.1M KCl on Cu-substrate.

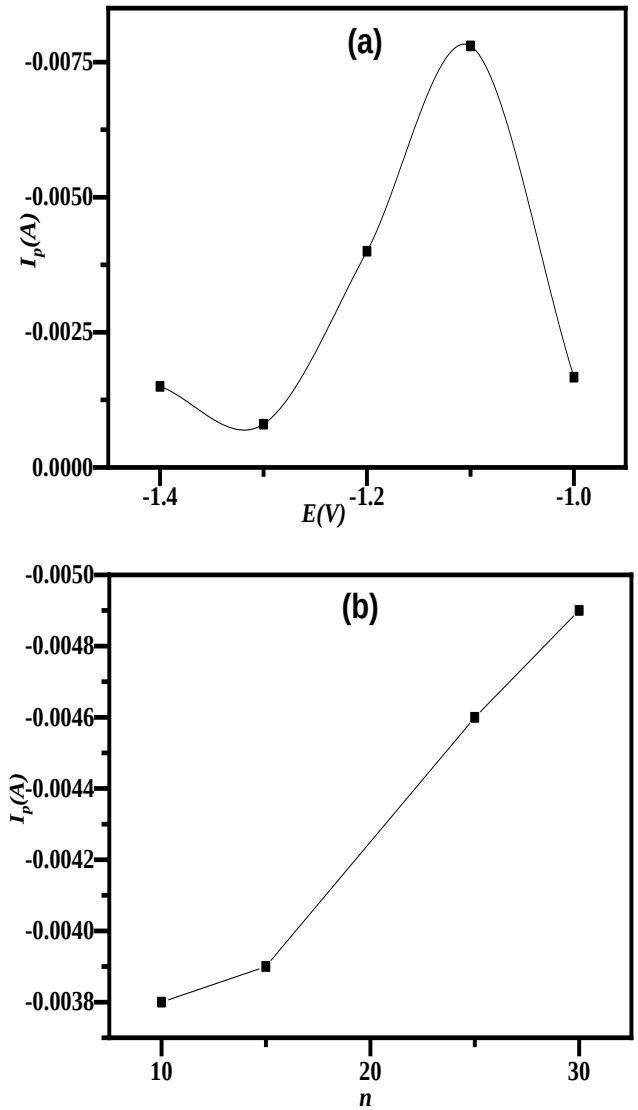

Fig. 9: CO_2 reduction peak current against (a) deposition potential and (b) deposition cycle number.

CRediT authorship contribution statement

Conceptualization, Mahmod Elrouby. and Hossnia S. Mohran; methodology, Amira Gelany; software, Amira Gelany.; validation, Mahmoud Elrouby; formal analysis, Amira; investigation, Hossnia S. Mohran; resources, Amira; data curation,Amira; writing—original draft preparation, Amira; writing—review and editing,Mahmoud; visualization, Hossnia S. Mohran ; supervision, Hossnia S. Mohran; All authors have read and agreed to the published version of the manuscript."

Data availability statement

The data used to support the findings of this study are available from the corresponding author upon request.

Declaration of competing interest

The authors declare that they have no known competing financial interests or personal relationships that could have appeared to influence the work reported in this paper.

References

[1] O. Echendu, S. Werta, F. Dejene, K. Egbo, *Journal of Alloys and Compounds*, 778 (2019) 197-203.
[2] M. El-rouby, A.S. Aliyev, *Journal of Materials Science: Materials in Electronics*, 25 (2014) 5618-5629.
[3] K. Erturk, S. Isik, O. Aras, Y. Kaya, *Optik*, 243 (2021) 167469.
[4] N. Nobari, M. Behboudnia, R. Maleki, *Materials Science and Engineering: B*, 224 (2017) 181-189.
[5] T.N. Swamy, A. Shelke, A. Lokhande, H. Pushpalatha, C. Lokhande, R. Ganesha, *Optik*, 138 (2017) 192-199.
[6] H. Salim, O. Olusola, A. Ojo, K. Urasov, M. Dergacheva, I. Dharmadasa, *Journal of Materials Science: Materials in Electronics*, 27 (2016) 6786-6799.
[7] J. Maricheva, S. Bereznev, R. Naidu, N. Maticiuc, V. Mikli, J. Kois, *Materials Science in Semiconductor Processing*, 54 (2016) 14-19.
[8] K. Deepa, N.L. Shruthi, M.A. Sunil, J. Nagaraju, *Thin Solid Films*, 551 (2014) 1-7.
[9] N.J. Ghdeeb, *Int. J. Thin. Film. Sci. Tec*, 11 (2022) 115-121.
[10] A. Hussain, J.T. Luo, P. Fan, G. Liang, Z. Su, R. Ahmed, N. Ali, Q. Wei, S. Muhammad, A.R. Chaudhry, *Applied Surface Science*, 505 (2020) 144597.
[11] M. Jeon, T. Shimizu, S. Shingubara, *Materials Letters*, 65 (2011) 2364-2367.
[12] A. Krishnan, D. Vidyadharan, S. Swaminathan, P. Kannan, *Materials Today: Proceedings*, 25 (2020) 122-128.
[13] P.U. Londhe, A.B. Rohom, N.B. Chaure, *Journal of Alloys and Compounds*, 771 (2019) 246-253.
[14] L. Lu, Y. Wang, X. Li, *Surface and Coatings Technology*, 212 (2012) 55-60.
[15] A. Ojo, I. Dharmadasa, *Materials Chemistry and Physics*, 180 (2016) 14-28.
[16] G. Riveros, C. Baez, D. Ramírez, C.J. Pereyra, R.E. Marotti, R. Romero, F. Martín, J.R. Ramos-Barrado, E.A. Dalchiele, *Journal of Alloys and Compounds*, 686 (2016) 235-244.
[17] J. Wellings, A. Samantilleke, S. Heavens, P. Warren, I. Dharmadasa, *Solar Energy Materials and Solar Cells*, 93 (2009) 1518-1523.
[18] R. Yu, T. Ren, C. Li, *Thin Solid Films*, 518 (2010) 5515-5519.
[19] K. Xie, Z. Wu, M. Wang, J. Yu, C. Gong, L. Sun, C. Lin, *Electrochemistry Communications*, 63 (2016) 56-59.
[20] Y. Yang, L. He, H. Xiang, *Russian Journal of Electrochemistry*, 42 (2006) 954-958.
[21] Q. Shen, J. Xue, J. Liu, X. Liu, H. Jia, B. Xu, *Solar Energy Materials and Solar Cells*, 136 (2015) 206-212.
[22] Q. Huang, K. Reuter, S. Amhed, L. Deligianni, L. Romankiw, S. Jaime, P.-P. Grand, V. Charrier, *Journal of The Electrochemical Society*, 158 (2010) D57.
[23] M. Mammadov, A.S. Aliyev, M. Elrouby, *International Journal of Thin Films Science and Technology*, 1 (2012) 42-53.